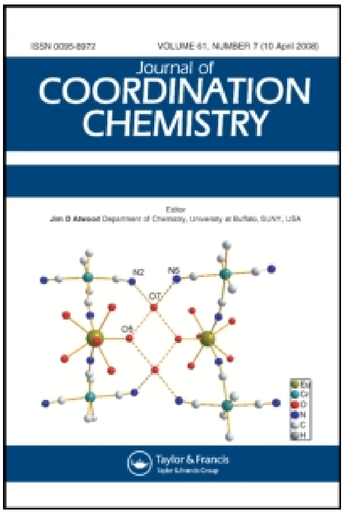

Journal of Coordination Chemistry
Publication details, including instructions for authors and subscription information:
http://www.informaworld.com/smpp/title~content=t713455674

Synthesis, characterization, and biological activity of metal complexes of azohydrazone ligand

Abdou S. El-Tabl[a]; Farag A. Aly[a]; Mohamad M. E. Shakdofa[b]; Adel M. E. Shakdofa[a]
[a] Faculty of Science, Department of Chemistry, El-Menoufia University, Shebin El-Kom, Egypt [b] Department of Inorganic Chemistry, National Research Center, Cairo, Egypt

First published on: 19 January 2010

To cite this Article El-Tabl, Abdou S. , Aly, Farag A. , Shakdofa, Mohamad M. E. and Shakdofa, Adel M. E.(2010) 'Synthesis, characterization, and biological activity of metal complexes of azohydrazone ligand', Journal of Coordination Chemistry, 63: 4, 700 — 712, First published on: 19 January 2010 (iFirst)

To link to this Article: DOI: 10.1080/00958970903545099

URL: http://dx.doi.org/10.1080/00958970903545099

Journal of Coordination Chemistry
Vol. 63, No. 4, 20 February 2010, 700–712

Synthesis, characterization, and biological activity of metal complexes of azohydrazone ligand

ABDOU S. EL-TABL*†, FARAG A. ALY†, MOHAMAD M.E. SHAKDOFA‡
and ADEL M.E. SHAKDOFA†

†Faculty of Science, Department of Chemistry, El-Menoufia University,
Shebin El-Kom, Egypt
‡Department of Inorganic Chemistry, National Research Center, P.O. 12622 Dokki,
Cairo, Egypt

(*Received 29 May 2009; in final form 21 September 2009*)

A new azohydrazone, 2-hydroxy-N′-2-hydroxy-5-(phenyldiazenyl)benzohydrazide (H_3L) and its copper(II), nickel(II), cobalt(II), manganese(II), zinc(II), cadmium(II), mercury(II), vanadyl(II), uranyl(II), iron(III), and ruthenium(III) complexes have been prepared and characterized by elemental and thermal analyses as well as spectroscopic techniques (^{1}H-NMR, IR, UV-Vis, ESR), magnetic, and conductivity measurements. Spectral data showed a neutral bidentate, monobasic bidentate, monobasic tridentate, and dibasic tridentate bonding to metal ions *via* the carbonyl oxygen in ketonic or enolic form, azomethine nitrogen, and/or deprotonated phenolic hydroxyl oxygen. ESR spectra of solid vanadyl(II) complex (**2**), copper(II) complexes (**3–5**), and (**7**) and manganese(II) complex (**10**) at room temperature show isotropic spectra, while copper(II) complex (**6**) shows axial symmetry with covalent character. Biological results show that the ligand is biologically inactive but the complexes exhibit mild effect on Gram positive bacteria (*Bacillus subtilis*), some octahedral complexes exhibit moderate effect on Gram negative bacteria (*Escherichia coli*), and VO(II), Cd(II), UO(II), and Hg(II) complexes show higher effect on Fungus (*Aspergillus niger*). When compared to previous results, metal complexes of this hydrazone have a mild effect on microorganisms due to the presence of the azo group.

Keywords: Metal complexes; Syntheses; Spectral; Azohydrazone; Magnetism; Biological activities

1. Introduction

Hydrazones are a special group of compounds in the Schiff base family characterized by the presence of >C=N–N=C<. The presence of two interlinked nitrogens separate them from imines, oximes, etc. Compared to simple hydrazone Schiff bases, acyl, aroyl, and hetero-aroyl Schiff bases have additional donor sites like >C=O, making them more flexible and versatile. This versatility has made hydrazones good polydentate chelating agents that can form a variety of complexes with various transition and inner transition metals. A number of hydrazone derivatives have interesting bioactivity such

---

*Corresponding author. Email: asaeltabl@yahoo.com

Journal of Coordination Chemistry
ISSN 0095-8972 print/ISSN 1029-0389 online © 2010 Taylor & Francis
DOI: 10.1080/00958970903545099

as antibacterial, antifungal [1], anticonvulsant [2], anti-inflammatory [3], antimalarial [4, 5], analgesic [5], antiplatelets, [6] antituberculosis [7], and anticancer activities [8]. Moreover, the copper(II) complex of salicylaldehyde benzoylhydrazone was shown to be a potent inhibitor of DNA synthesis and cell growth [9]. Some hydrazone analogues have been investigated as potential oral iron chelating drugs for the treatment of genetic disorders such as thalassemia [10] and have also been suggested as possible metal chelating agents for treating neurodegenerative disorders such as Alzheimer disease [11]. Hydrazones also act as herbicides, insecticides, nematocides, rodenticides, and plant growth regulators, and are used as plasticizers and stabilizers for polymers, polymerization initiators, antioxidants, etc. Hydrazone derivatives are used in analytical chemistry as selective metal extracting agents as well as in the spectroscopic determination of certain transition metals [12]. In the present work a new azohydrazone ligand and its copper(II), nickel(II), cobalt(II), manganese(II), zinc(II), cadmium(II), mercury(II), vanadyl(II), uranyl(II), iron(III), and ruthenium(III) complexes have been prepared and characterized.

2. Experimental

The starting chemicals were of analytical grade from Merck. 2-Hydroxy-N′-2-hydroxy-5-(phenyldiazenyl)benzohydrazide was prepared by a published method [13]. Elemental analyses were determined by the Analytical Unit of Cairo University, Egypt. Standard analytical methods were used to determine the metal ion content [14]. All metal complexes were dried in vacuum over anhydrous $CaCl_2$. IR spectra were measured using a JASCO FT/IR 6100 spectrophotometer (400–4000 cm^{-1}). Electronic spectra in DMF were recorded on a Perkin-Elmer 550 spectrophotometer. The molar conductances of 10^{-3} M solution of the complexes in DMSO were measured at 25°C with a Bibby conductometer-type MCl. The resistance was measured in ohms and the molar conductivities were calculated according to the equation: $\Lambda = V \times K \times Mw/g \times \Omega$, where Λ = molar conductivity ($ohm^{-1}\,cm^2\,mol^{-1}$), V = volume of the complex solution, K = cell constant 0.92 cm^{-1}, Mw = molecular weight of the complex, g = weight of the complex, and Ω = resistance measured in ohms. ^{1}H-NMR spectra of the ligand and its zinc(II) and uranyl(II) complexes in d_6-DMSO were recorded using a JEOL EX-270 MHz FT-NMR spectrometer. Thermal analysis (TG) was carried out in nitrogen on a Shimadzu DT-30 thermal analyzer from room temperature to 800°C at a heating rate of 10°C min^{-1}. Magnetic moments were measured using the Gouy method ($\mu_{eff} = 2.84(\chi_M^{corr} \times T)^{1/2}$) [15]. ESR measurements of solid complexes at room temperature were made using a Varian E-109 spectrophotometer with DPPH as a standard material. TLC was used to confirm the purity of the compounds.

2.1. *Preparation of ligand [H_3L]*

The azohydrazone ligand was prepared (figure 1) by adding equimolar amounts of 2-hydroxy benzohydrazide (1.52 g, 1.0 mmol in 20 mL of absolute ethanol) to 2-hydroxy-N′-2-hydroxy-5-(phenyldiazenyl)benzohydrazide) (2.26 g, 1.0 mmol in 20 mL of absolute ethanol). The mixture was refluxed while stirring for 1 h. The formed solid

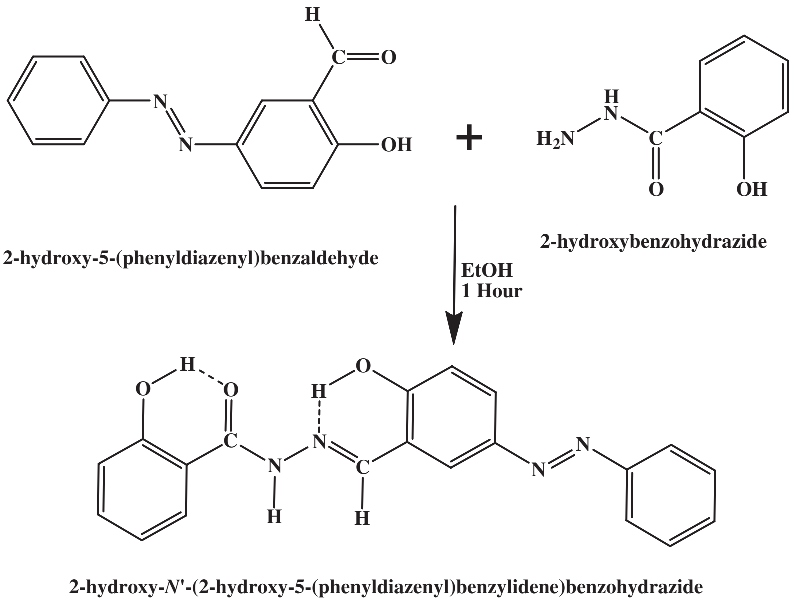

Figure 1. Preparation of ligand H_3L.

product was filtered off, washed with cold ethanol several times, followed by crystallization from ethanol and finally dried under vacuum over anhydrous $CaCl_2$.

2.2. *Preparation of metal complexes 2–16*

Metal complexes were prepared by mixing a hot ethanolic solution of the metal acetate, $M(CH_3COO)_2 \cdot nH_2O$ – where M = Cu(II), Ni(II), Co(II), Mn(II), Zn(II), Cd(II), Hg(II), or UO_2(II), metal chloride – $CuCl_2 \cdot 2H_2O$, $FeCl_3 \cdot 6H_2O$, $RuCl_3 \cdot 2H_2O$ or metal sulphate – $CuSO_4 \cdot 5H_2O$, $VOSO_4 \cdot H_2O$, or $Cu(NO_3)_2 \cdot 2.5H_2O$ with a suitable amount of a hot ethanolic solution of the ligand to form 1 : 1 or 1 : 2 M/L (metal/ligand) complexes in the presence of triethylamine (TEA). The reaction mixture was then refluxed for a time depending on the metal salt used. The precipitates formed were filtered off, washed with ethanol, then with diethyl ether, and dried under vacuum over anhydrous $CaCl_2$.

2.3. In-vitro *antibacterial and antifungal activities*

The biological activities of the hydrazone and its metal complexes were carried out in the Faculty of Science, Botany Department, Laboratory of Microbiology, El-Menoufia University, Egypt, by disc diffusion method [16, 17]. The antibacterial activities were done using the following organisms: *Escherichia coli*, *Bacillus subtilis* and *Aspergillus niger* for antifungal activity at $10\,\mathrm{mg\,mL^{-1}}$ concentrations in solvent DMSO, with DMSO as a negative control. The bacteria were subcultured in nutrient agar medium prepared using peptone, beef extract, NaCl, agar agar, and distilled water. The Petri dishes were incubated for 48 h at 37°C. Standard antibacterial drug (tetracycline) was also screened under similar conditions for comparison. The fungus was subcultured in Dox's medium, prepared using yeast extract, sucrose, $NaNO_3$, agar agar, KCl, KH_2PO_4, $MgSO_4 \cdot 7H_2O$, distilled water, and a trace of $FeCl_3 \cdot 6H_2O$. Standard antifungal drug (amphotricene B) was used for comparison. The Petri dishes were incubated for 48 h at 28°C. The zone of inhibition was measured in millimeters. All determinations were made in duplicate for each compound.

3. Results and discussion

The ligand 2-hydroxy-N′-2-hydroxy-5-(phenyldiazenyl)benzohydrazide (H_3L) and its metal complexes **1–16** are stable at room temperature, non-hygroscopic, insoluble in common organic solvents such as ethanol, methanol, chloroform, and acetone but completely soluble in DMF and DMSO. Elemental analyses showed that all complexes were composed of ligand and metal ions with a molar ratio of 2 : 1 except **7**, **15**, and **16** with molar ratio of 1 : 1.

3.1. *IR spectra*

The most important bands of the ligand and its metal complexes are presented in table 1. The spectrum of the ligand (H_3L) showed a strong band at $1662\,cm^{-1}$ assigned to carbonyl of the hydrazide, and a medium band at $3190\,cm^{-1}$ assigned to υ(NH) [18, 19], indicating that the ligand is present in the ketonic form in the solid state [20–22]. The spectrum showed two broad bands at 3200–3550 and $2500–3100\,cm^{-1}$ assigned to the stretching vibration of the phenolic hydroxyl groups with intra- and intermolecular hydrogen bonding [19, 20]. Relatively strong and medium bands at 1618, 1454, and $921\,cm^{-1}$ may be assigned to azomethine [19, 23], azo [24], and υ(N–N) [19], respectively. Bands at 1277 and $1302\,cm^{-1}$ may be assigned to the υ(C–OH) of the phenolic moieties [22, 25]. A comparison of the spectra of the complexes shows the bonding between the ligand and the metal ions. For spectra of **3**, **7**–**10**, and **13**–**15**, disappearance of bands characteristic to υ(C=O) and υ(NH) indicate that bonding in enol is formed through the enolic carbonyl oxygen. This mode of bonding is supported by the appearance of new bands in the 1491–1521 and $1236–1254\,cm^{-1}$ ranges, assigned to υ(N=C–O) and υ(C–O), respectively [26]. For **2**, **4**–**6**, **11**, **12**, and **16** the band characteristic of υ(NH) is still present and the band of the carbonyl shifts to lower frequency by $4–55\,cm^{-1}$, indicating coordination in its ketonic form *via* the carbonyl. In all complexes the band characteristic of azomethine shifted to lower frequency ($1541–1605\,cm^{-1}$). In **3**, **7**–**10**, and **13**–**15** there is an additional band at $1560–1624\,cm^{-1}$ assigned to υ(N=C–C=N) [26]; the band characteristic to υ(N–N) shifted to higher frequency. Increasing the frequency of υ(N–N) is a clear indication of increasing double bond character and coordination *via* the azomethine group [23]. New bands in the 601–690, 530–587, and $461–529\,cm^{-1}$ ranges for **2**–**16** may be assigned to υ(M–O), υ(M $\leftarrow$ O), and υ(M $\leftarrow$ N), respectively [26].

3.1.1. Anions. The IR spectrum of the nitrate complex (**5**) showed bands at υ_5(1446), υ_1(1308), and υ_2(1023) indicating that they were nitrate coordinated. The difference

Table 1. The IR spectral (cm^{-1}) assignments for H_3L and metal complexes.

Compound no.	Ligand/complexes	OH/H_2O	NH	C=O	C=N/C=N–N=C	N=C–O	N=N	C–OH	C–O	N–N	M–O	M–N
1	$C_{20}H_{16}N_4O_3(H_3L)$	3200–3550 2500–3100	3190	1662	1618	–	1454	1302, 1277	–	921	–	–
2	$[VO(H_3L)_2(H_2O)]\cdot(SO_4)$	3432(br)	3176	1656	1605	–	1445	1290, 1265	–	963	530	510
3	$[Cu(H_2L)_2(H_2O)_2]\cdot C_2H_5OH$	3450(br)	–	–	1621, 1595	1519	1447	1300, 1274	1236	956	625, 553	498
4	$[Cu(H_3L)_2Cl_2]$	3427(br)	3208, 3151	1617	1590	–	1455	1307, 1270	–	964	563	529
5	$[Cu(H_3L)_2(NO_3)_2]$	3433(br)	3105	1621	1599	–	1446	1308, 1281	–	948	543	477
6	$[Cu(H_3L)_2(SO_4)]\cdot 2H_2O$	3433(br)	3190	1627	1595	–	1447	1307, 1273	–	957	559	472
7	$[Cu(HL)(H_2O)]$	3423(br)			1604	1491	1450	1310, 1290	1242	950	682, 578	507
8	$[Ni(H_2L)_2]\cdot 3H_2O$	3394(br)	–	–	1600, 1576	1510	1467	1315, 1297	1245	953	689, 569	507
9	$[Co(H_2L)_2]\cdot 4H_2O$	3397(br)	–	–	1603, 1568	1513	1465	1320, 1286	1248	956	690, 572	505
10	$[Mn(H_2L)_2]\cdot 3H_2O$	3443(br)	–	–	1598, 1573	1510	1464	1319, 1290	1254	959	689, 567	501
11	$[Fe(H_2L)_2]Cl\cdot 2H_2O\cdot C_2H_5OH$	3418(br)	3209	1607	1541	–	1457	1302, 1250	–	960	657, 567	529
12	$[Ru(H_2L)_2]Cl\cdot 4H_2O$	3432(br)	3204	1616	1549	–	1455	1303, 1259	–	969	601, 563	461
13	$[Zn(H_2L)_2]\cdot 3H_2O$	3444(br)	–	–	1624, 1577	1517	1467	1322, 1282	1249	960	682, 573	506
14	$[Cd(H_2L)_2]\cdot 3H_2O$	3450(br)	–	–	1615, 1560	1515	1464	1313, 1285	1251	959	682, 563	498
15	$[(UO_2)(HL)]\cdot H_2O$	3421(br)	–	–	1606, 1572	1521	1467	1320, 1291	1247	962	683, 587	493
16	$[Hg(H_2L)(OAc)(H_2O)_2]$	3433(br)	3176	1655	1589	–	1467	1290, 1251	–	959	687, 539	491

between the two high bands (υ_5–υ_1) is 138 cm^{-1}, indicating a unidentate nitrate [27, 28]. For sulfate complexes (**2** and (**6**) there are new bands at 1146, 1008 and 655, and 1239, 1121, 1025, and 918 cm^{-1} for the two complexes, respectively. The bands of **2** confirm ionic sulfate [27, 29], further confirmed by conductance; bands of **6** indicate that sulfate is chelating bidentate [27, 30]. The $\upsilon_{as}(CO^{2-})$ and $\upsilon_s(CO^{2-})$ of free acetate are *ca* 1560 and 1416 cm^{-1}, respectively. In unidentate acetate complexes, υ(C=O) is higher than $\upsilon_s(CO^{2-})$ and υ(C–O) is lower than $\upsilon_{as}(CO^{2-})$. As a result the separation between the two υ(CO) is much larger in unidentate than in free ion but bidentate has less separation than in the free ion, while for bridging bidentate the two υ(CO) are close to the free ion [27]. In **16** there are two new bands at 1547 and 1358 cm^{-1} attributed to symmetric and asymmetric stretching of acetate. The difference of 189 cm^{-1} indicates that the acetate is unidentate [26, 31]. Infrared spectra of the vanadyl and uranyl complexes (**2** and **15**) reveal medium bands at 914 and 913 cm^{-1} attributed to υ(V=O) [32] and υ(O=U=O) [26], respectively.

3.2. *^{1}H-NMR spectra*

The ^{1}H-NMR spectral data of the ligand and its uranyl(II) and uranyl complexes confirm the suggested binding of the ligand with the metal ions. H_3L shows no signal of the amino group ($-NH_2$) characteristic to the starting material (hydrazide). The spectrum shows singlets at 12.13 (s, 1H), 11.78 (s, 1H), and 11.76 (s, 1H) ppm which may be assigned to the hydroxyl proton (OH) and (NH) protons, respectively [18–21]; a singlet at 8.81 (s, 1H) ppm assigned to azomethine proton (H–C=N) [19, 21]; and multiplets in the 6.98–8.26 (m, 12H) ppm range attributed to aromatic protons [33]. The ligand exhibits the keto form only with no evidence for the enol form [20]. ^{1}H NMR spectra of the zinc complex (**13**) and uranyl complex (**15**) show no signal characteristic to NH; singlets at 13.58 (s, 2H) and 13.58 (s, 1H) for the two complexes, respectively, may be assigned to the hydroxyl (OH) protons [18–21], singlets at 8.73 and 9.53 (s, 1H) ppm assigned to azomethine proton (H–C=N) [19, 21]; and multiplets in the 7.06–8.41 (m, 12H) ppm range attributed to aromatic protons [33]. Comparison of spectra of **13** and **15** with the free ligand indicate enolic form in **13**, but the absence of signal of (NH) and one (OH) indicates a dibasic ligand *via* the enolic carbonyl and deprotonated hydroxyl in **15**.

The infrared spectra, ^{1}H-NMR, and elemental analyses reveal that ligand bonded in four modes, neutral bidentate coordinated *via* oxygen of carbonyl in the ketonic form and nitrogen of the azomethine (**2** and **4**–**6**), monobasic bidentate *via* carbonyl oxygen in the enolic form and nitrogen of the azomethine (**3**, **8**–**10**, **13** and **14**), monobasic tridentate *via* carbonyl in the ketonic form, nitrogen of azomethine and deprotonated hydroxyl oxygen of azo moiety (**11**, **12** and **16**), and dibasic tridentate *via* the carbonyl in enolic form, deprotonated hydroxyl, and azomethine nitrogen (**7** and **15**).

3.3. *Mass spectrum of the ligand*

The mass spectrum of H_3L revealed molecular ion peak at m/z 361, consistent with the formula weight (360.37), confirming the identity. The ligand splits to several fragments which possess ion peaks at $m/z = 240$, 224, 163, 148, 135, 121, 105, 93, and 77, corresponding to $C_{14}H_{12}N_2O_2$, $C_{14}H_{12}N_2O$, $C_8H_7N_2O_2$, $C_8H_8N_2O$, $C_7H_7N_2O^-$, C_7H_7NO, $C_7H_5O^-$, C_6H_7N, and $C_7H_5^-$, respectively.

Table 2. The electronic absorption spectra (extinction coefficients) and magnetic moments for H_3L and its complexes.

Compound no.	Bands in DMSO (Є $mol^{-1} cm^{-1}$)	μ_{eff} (BM)
1	240(448), 270(479), 326(4280), 346(5658), 400(7961), 465(1932)	–
2	245(1294), 265(984), 325(3589), 360(4933), 400(4041), 470(5402), 490(2616), 520(723), 680(53)	1.66
3	240(1955), 255(2777), 270(1187), 340(1296), 380(1590), 405(6726), 640(268)	1.71
4	245(1412), 265(1213), 340(2082), 380(1710), 400(1581), 485(160), 655(221)	1.68
5	235(1650), 270(1722), 335(302), 360(339), 405(379), 460(411), 675(113)	1.66
6	240(374), 270(354), 340(982), 365(2045), 400(2677), 480(330), 640(343)	1.70
7	240(1445), 266(880), 326(716), 344(735), 398(1445), 475(961), 668(344), 764(92)	1.81
8	240(396), 265(5545), 350(2647), 380(2537), 415(3776), 465(2097), 520(861), 650(75), 960(28)	2.89
9	235(1925), 270(2605), 330(1207), 365(1006), 410(1622), 455(1026), 500(1376), 650(311), 980(22)	4.11
10	240(1173), 280(5952), 355(970), 385(880), 410(1331), 465(971), 500(751), 560(75), 610(29)	4.82
11	255(1351), 285(2947), 330(2721), 390(3202), 430(1754), 455(854), 580(4578), 667(2661)	5.12
12	255(494), 270(1100), 320(1725), 380(1376), 435(553), 465(431), 575(3919), 650(2548)	1.68
13	235(1626), 285(2568), 335(1539), 370(1585), 420(2568), 460(1619)	Diamagnetic
14	250(2087), 285(2789), 340(1587), 385(1395), 425(1991), 470(1508)	Diamagnetic
15	245(1348), 285(2000), 330(654), 3875(903), 415(699), 475(886), 530(1155)	Diamagnetic
16	245(1291), 270(1357), 330(597), 370(460), 405(293), 485(134)	Diamagnetic

Є is molar extinction coefficient ($mol^{-1} cm^{-1}$).

3.4. *Molar conductivity*

The molar conductivity of 1×10^{-3} M solution of **3–10** and **13–16** in DMSO at room temperature are in the $9.1:28\,\Omega^{-1}\,cm^2\,mol^{-1}$ range, indicating nonelectrolytes. Complexes **2**, **11**, and **12** have values 90, 74.5, and $81.5\,\Omega^{-1}\,cm^2\,mol^{-1}$, respectively, indicating the electrolytic nature of these complexes [26, 34].

3.5. *Magnetic moments*

The magnetic moments of **2–12** at room temperature (table 2) show that all these complexes are paramagnetic. The vanadyl complex (**2**) shows 1.66 BM corresponding to one unpaired electron [26]. Copper(II) complexes (**3–7**) show values from 1.66 to 1.81 BM, consistent with one unpaired electron in octahedral or square planar structure [20]. Complex **8** shows 2.89 BM consistent with two unpaired electrons, indicating octahedral nickel(II) [20]. Cobalt(II) complex **9** shows 4.11 BM, indicating high-spin cobalt(II) [35]. The magnetic moment values of manganese(II) and iron(III) complexes (**10** and **11**) are 4.82 and 5.12 BM, respectively, compatible with high-spin manganese(II) and iron(III) complexes [35]. The magnetic moment of ruthenium(III) complex **12** is 1.68 BM characteristic to d^5 low-spin ruthenium(III) [35].

3.6. *Electronic spectra*

Electronic absorption bands of the ligand and its metal complexes in DMSO from 200 to 1100 nm are reported in table 2. The ligand has three sets of bands in the UV and visible regions [36]. The first at 240 and 270 nm may be assigned to $\pi \rightarrow \pi^*$ transitions in the aromatic and intra ligand $\pi \rightarrow \pi^*$ transition [20, 35]. The second set at 326 and 355 nm may be assigned to $n \rightarrow \pi^*$ of the azomethine and carbonyl group [20]. The third set at 400 nm corresponds to $\pi \rightarrow \pi^*$ transition involving the π electron of the azo group [36, 37]. A band located in the visible region at 465 nm can be assigned to $\pi \rightarrow \pi^*$ transition involving the whole electronic system with considerable charge transfer character arising mainly from the phenolic moiety [36, 37]. The electronic spectrum of **2** in DMSO solution showed bands at 685, 520, and 490 nm which may be assigned to ${}^2B_2(\mathrm{d}_{xy}) \rightarrow E(\mathrm{d}_{xz},\mathrm{d}_{zy})$, ${}^2B_2(\mathrm{d}_{xy}) \rightarrow {}^2B_1(\mathrm{d}_{x^2-y^2})$, and ${}^2B_2(\mathrm{d}_{xy}) \rightarrow {}^2A_1(\mathrm{d}_{z^2})$, indicating that vanadyl(II) has a distorted octahedral structure (figure 2) [38–40]. Spectra of copper(II)

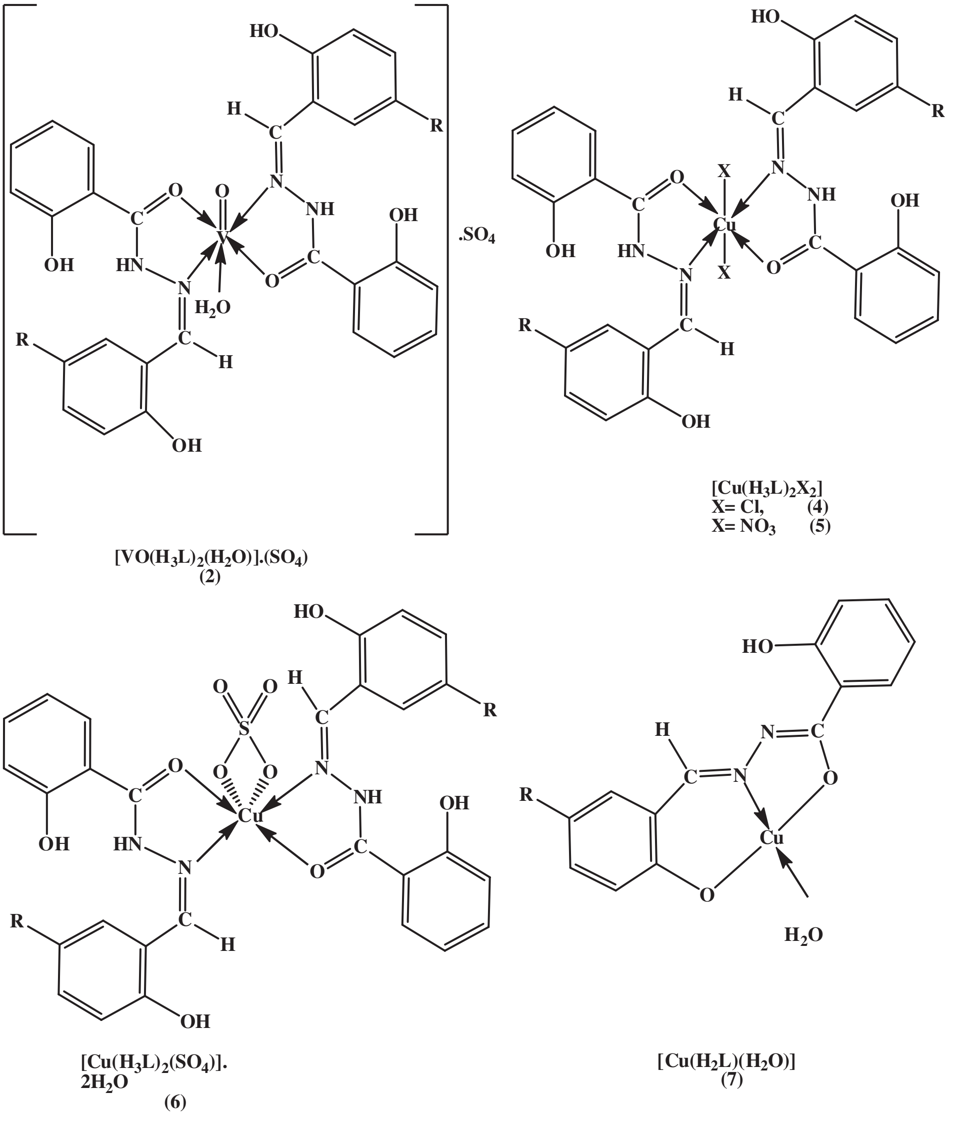

$[VO(H_3L)_2(H_2O)].(SO_4)$
(2)

$[Cu(H_3L)_2X_2]$
X= Cl, **(4)**
X= NO_3 **(5)**

$[Cu(H_3L)_2(SO_4)]$.
$2H_2O$
(6)

$[Cu(H_2L)(H_2O)]$
(7)

Figure 2. Structural representation of the metal complexes.

complexes (**3–7**) showed that **3–6** were nearly identical with a broad band centered at 640–675 nm. The position and the broadness of this band indicated that copper(II) has tetragonally distorted octahedral geometry (figure 2). This broad band consists of three superimposed transitions $^2B_{1g} \rightarrow {}^2E_g$, $^2B_{1g} \rightarrow {}^2A_{1g}$, and $^2B_{1g} \rightarrow {}^2B_{2g}$ [38, 41]. However, the electronic spectrum of **7** shows a broad band at 668 with a shoulder at 764 nm, similar to square planar copper(II) complexes (figure 2) [38, 42]. The nickel(II) complex (**8**) exhibits three bands at (υ_1) 960, (υ_2) 650, and (υ_3) 520 nm assigned to $^3A_{2g} \rightarrow {}^3T_{2g}$, $^3A_{2g} \rightarrow {}^3T_{1g}$, and $^3A_{2g} \rightarrow {}^3T_{1g}(p)$, characteristic to octahedral nickel(II) (figure 2) [38, 42, 43]. The υ_2/υ_1 ratio is 1.48, less than the usual range 1.5–1.75, indicating distorted nickel(II) [37, 43, 44]. Cobalt(II) complex (**9**) showed three bands at 980, 650, and 500 nm assigned to $^4T_{1g}(F) \rightarrow {}^4T_{2g}(F)$ (υ_1), $^4T_{1g} \rightarrow {}^4A_{2g}(\upsilon_2)$, and $^4T_{1g}(F) \rightarrow {}^4T_{1g}(p)$

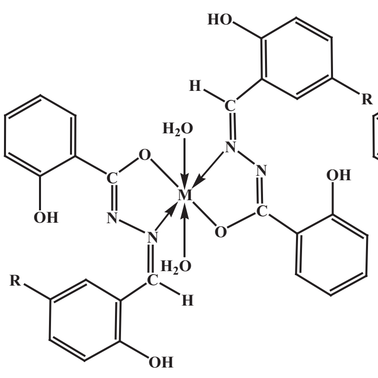

$[M(H_2L)_2(H_2O)_2].nX$
M= Cu(II), X= C_2H_5OH, n= 0 (3)
M= Ni(II), X= H_2O, n= 3 (8)
M= Co(II), X= H_2O, n= 4 (9)
M= Mn(II), X= H_2O, n= 3 (10)
M= Zn(II), X= H_2O, n= 3 (13)
M= Cd(II), X= H_2O, n= 3 (14)

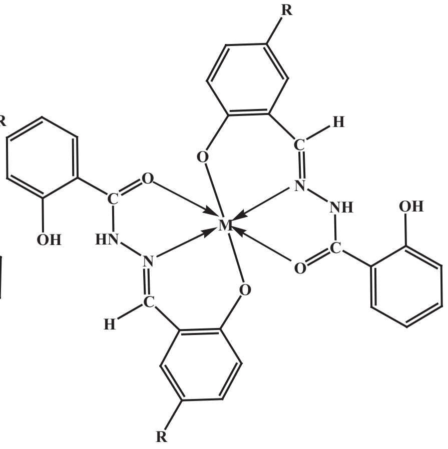

$[M(H_2L)_2]Cl.nH_2O.mC_2H_5OH$
M= Fe, n= 2,m= 1 (11)
M=Ru, n= 4, m= 0 (12)

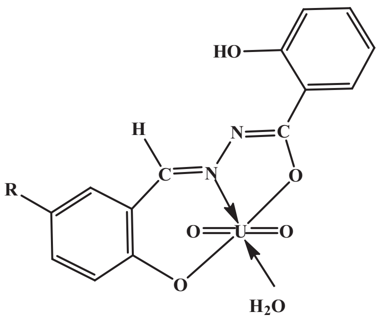

$[UO_2(HL)(H_2O)]$
(15)

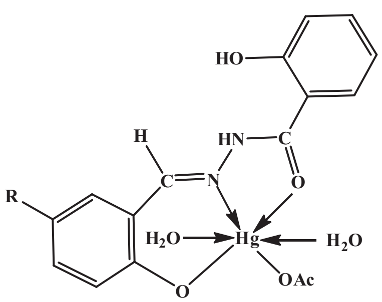

$[Hg(H_2L)(OAc)(H_2O)_2]$
(16)

R =

Figure 2. Continued.

(υ_3), respectively, suggesting octahedral geometry around cobalt(II) (figure 2) [38, 45, 46]. The ratio of $\upsilon_2/\upsilon_1 = 1.51$, lower than for an octahedral cobalt(II) (1.95–2.48), indicates distorted octahedral structure [45]. The manganese(II) complex (**10**) displays weak absorptions at 610, 560, 500, and 465 nm assigned to ${}^6A_{1g} \rightarrow {}^4T_{1g}$ (${}^4G$) (υ_1), ${}^6A_{1g} \rightarrow {}^4E_g$ (${}^4G$) (υ_2), ${}^6A_{1g} \rightarrow {}^4E_g$ (${}^4D$) (υ_3), and ${}^6A_{1g} \rightarrow {}^4T_{1g}$ (${}^4p$) (υ_4), respectively, characteristic to manganese(II) in octahedral geometry (figure 2) [47]. The iron(III) complex (**11**) shows bands at 667 and 580 nm assigned to ${}^6A_{1g} \rightarrow {}^4T_{2g}(G)$ and ${}^6A_1(G) \rightarrow {}^4T_1(G)$ transitions, characteristic of octahedral iron(III) (figure 2) [48]. Ruthenium(III) complex **12** displays bands at 650 and 575 nm assigned to ${}^2T_{2g} \rightarrow {}^4T_{1g}$, ${}^2T_{2g} \rightarrow {}^4T_{2g}$ transitions, characteristic of octahedral ruthenium(III) (figure 2) [49]. The uranyl complex (**15**) exhibits one band at 530 nm assigned to ligand to uranium charge transfer [50]. The zinc(II), cadmium(II), and mercury(II) complexes (**13–16**) show intraligand transitions (table 2).

3.7. *Electron spin resonance*

The electron spin resonance (ESR) spectrum of **2** (d^1, ${}^{51}V$, $I = 7/2$) is not resolved at room temperature, showing an isotropic signal at 2.11 [51, 52]. ESR spectra of **3–5** and **7** at room temperature exhibit signals at high field, which are isotropic due to tumbling with g_{iso} values of 2.06, 2.11, 2.07, and 2.07, respectively [32, 53]. The ESR spectrum of polycrystalline **6** at room temperature is characteristic for d^9 configuration having an axial symmetry with $d_{(x^2-y^2)}$ ground state [54, 55]. The g values $g_\parallel = 2.29$, $g_\perp = 2.07$ with $g_{iso} = 2.16$ suggest elongated tetragonal octahedral structure [56]. The $g_\parallel > g_\perp > g_{e(2.0023)}$ confirm tetragonal distortion around copper(II) [57–59]. The $g_\parallel/A_\parallel$ value is diagnostic of the stereochemistry [58] with range 105–135 cm^{-1} for square planar and 150–250 cm^{-1} for tetragonally distorted complexes. The $g_\parallel/A_\parallel$ for **6** is 178.5, indicating a tetragonal distorted octahedral complex [58–60]. Exchange coupling interaction between the copper(II) ions with $G = 4.29$ confirmed tetragonal octahedral structure [61, 62]. The in plane σ-covalencey parameter α^2 was calculated [61–65].

$$\alpha^2 = -A_\parallel/0.036 + (g_\parallel - 2.0023) + (g_\perp - 2.0023) + 0.04$$

If $\alpha^2 = 1$, the bond would be completely ionic and if $\alpha^2 = 0.5$, the bond would be completely covalent; the α^2 value reported here is 0.72 suggesting considerable covalent bonding character. ESR spectra of **8** and **9** at room temperature do not show ESR spectral signals because the rapid spin lattice relaxation of the nickel(II) and cobalt(II) broadens the lines at higher temperature [35]. The ESR spectrum of solid **10** at room temperature gives an isotropic signal centered at 2.06, broadened due to spin relaxation [35].

3.8. *Thermal analyses (DTA and TG)*

The thermogravimetric analysis TG was measured in the temperature range 20–800°C under nitrogen and the results are shown in "Supplementary material". The complexes are generally decomposed in several steps. The first step is the elimination of the water of hydration or solvent as in **3** which lost ethanol at 21–47°C, **9** lost water at 25–105°C and iron(III) complex lost ethanol and water at 25–61°C. The second step is the elimination of water of coordination, as in **2**, **3**, **7**, and **9** in the temperature range of

Table 3. Biological activities of the ligand and its metal complexes against bacteria and fungi.

	Inhibition zone in mm		
Compounds	*A. niger*	*E. coli*	*B. subtilis*
DMSO	0	0	0
Amphotricene B	16	–	–
Tetracyclene	–	35	40
1	0	0	0
2	13	0	14
3	0	10	12
4	0	0	14
5	0	0	16
6	0	0	12
7	0	0	11
8	0	20	18
9	0	17	17
10	0	11	12
11	0	0	0
12	0	0	16
13	0	10	15
14	16	20	18
15	17	10	16
16	34	17	21

110–370°C. The third step is the loss of anions (sulfate, nitrate, and chloride) (H_2SO_4, HCl, and HNO_3) from 200°C to 380°C in **2**, **4**, **5**, and **11**. The fourth step is complete decomposition of the complexes through degradation of the ligand at 300–570°C leaving the metal oxide. Analysis of **3** indicates the following decomposition patterns:

$$[Cu(H_2L)_2(H_2O)_2]\cdot C_2H_5OH \xrightarrow{20-47^{\circ}C} [Cu(H_2L)_2(H_2O)_2]$$

$$[Cu(H_2L)_2(H_2O)_2] \xrightarrow{330-370^{\circ}C} [Cu(H_2L)_2]$$

$$[Cu(H_2L)_2] \xrightarrow{390-430^{\circ}C} CuO$$

3.9. *Antibacterial and antifungal screening*

The microbial results of the hydrazone and its metal complexes are provided in table 3. The metal complexes exhibit inhibitory effects toward the activity of Gram-positive bacterium (*B. subtilis*) while **3**, **8–10**, and **13–16** exhibit inhibitory effects toward Gram-negative bacterium and **2** and **14–16** toward the fungus (*A. niger*); the ligand is biologically inactive under the experimental conditions. Plots of the bioactivity are provided in "Supplementary material". The most interesting point of biological measurement is that the azohydrazone is biologically inactive while other types of hydrazones such as phenylamino acetoacetylacetone hydrazone [66], 2-acetylpyridine [N-(3-hydroxy-2-naphthoyl)] hydrazone [67], *p*-amino acetophenone isonicotinoyl hydrazone [68], and Schiff bases [69–72] are biologically strongly active. Also, their metal complexes show enhanced biological activity over azohydrazone complexes. The lower activity of azohydrazone and its complexes against both bacteria and fungi may be attributed to the presence of the azo group.

4. Conclusion

Metal complexes of 2-hydroxy-N′-2-hydroxy-5-(phenyldiazenyl)benzohydrazide (H_3L) have been prepared and characterized by elemental and thermal analyses as well as spectroscopic techniques. The complexes are form in the molar ratio of 2L : 1M except **7**, **15**, and **16**. The ligand is neutral bidentate, monobasic bidentate, monobasic tridentate, or dibasic tridentate, bonded *via* the oxygen of carbonyl, nitrogen of the azomethine, or deprotonated hydroxyl oxygen of azo moiety. Electronic spectra reveal distorted octahedral except **7** with square planar geometry. The ESR spectrum of **6** confirms tetragonally distorted octahedral geometry with covalent bond character. The biological results show the ligand to be biologically inactive but the complexes exhibit mild effect on *B. subtilis* and some octahedral complexes exhibit a moderate effect on *E. coli*. Complexes of VO(II), Cd(II), UO(II), and Hg(II) show higher effect on *A. niger*. Comparing to previous results, the metal complexes of this type of hydrazone have mild effect on microorganisms studied due to the presence of the azo group.

References

[1] C. Loncle, J.M. Brunel, N. Vidal, M. Dherbomez, Y. Letourneux. *Eur. J. Med. Chem.*, **39**, 1067 (2004).
[2] Ş.G. Küçükgüzel, A. Mazi, F. Sahin, S. Öztürk, J. Stables. *Eur. J. Med. Chem.*, **38**, 1005, (2003).
[3] R. Todeschini, A.L.P. de Miranda, K.C.M. da Silva, S.C. Parrini, E.J. Barreiro. *Eur. J. Med. Chem.*, **33**, 189 (1998).
[4] P. Melnyk, V. Leroux, C. Sergheraert, P. Grellier. *Bioorg. Med. Chem. Lett.*, **16**, 31 (2006).
[5] P.C. Lima, L.M. Lima, K.C.M. da Silva, P.H.O. Léda, A.L.P. de Miranda, C.A.M. Fraga, E.J. Barreiro. *Eur. J. Med. Chem.*, **35**, 187 (2000).
[6] C. Cunha, J.M. Figueiredo, J.L.M. Tributino, A.L.P. Miranda, H.C. Castro, R.B. Zingali, C.A.M. Fraga, M.C.B.V. de Souza, V.F. Ferreira, E.J. Barreiro. *Bioorg. Med. Chem.*, **11**, 2051 (2003).
[7] K.K. Bedia, O. Elçin, U. Seda, K. Fatma, S. Nathaly, R. Sevim, A. Dimoglo. *Eur. J. Med. Chem.*, **41**, 1253 (2006).
[8] N. Terzioglu, A. Gürsoy. *Eur. J. Med. Chem.*, **38**, 781 (2003).
[9] E.W. Ainscough, A.M. Brodie, A.J. Dobbs, J.D. Ranford, J.M. Waters. *Inorg. Chim. Acta*, **267**, 27 (1998).
[10] J.L. Buss, B.T. Greene, J. Turner, F.M. Torti, S.V. Torti. *Curr. Top. Med. Chem.*, **4**, 1623 (2004).
[11] P.S. Donnelly, A. Caragounis, T. Du, K.M. Laughton, I. Volitakis, R.A. Cherny, R.A. Sharples, A.F. Hill, Q.-X. Li, C.L. Masters, K.J. Barnham, A.R. White. *J. Biol. Chem.*, **283**, 4568 (2008).
[12] P.B. Sreeja, A. Sreekanth, C.R. Nayar, M.R.P. Kurup, A. Usman, I.A. Razak, S. Chantrapromma, H.K. Fun. *J. Mol. Struct.*, **645**, 221 (2003).
[13] J.-N. Liu, B.-W. Wu, B. Zhang, Y. Liu. *Turk. J. Chem.*, **30**, 41 (2006).
[14] G. Svehla. *Vogel's Textbook of Macro and Semi Micro Quantitative Inorganic Analysis*, 5th Edn, Longman Inc., New York (1979).
[15] M. Massaccsi, R. Pinna, G. Poticelli. *Spectrochim. Acta, Part A*, **38**, 725 (1982).
[16] E.O. Offiong, S. Martelli. *I. L. Farm.*, **49**, 513 (1994).
[17] G. Collee, J.P. Duguid, A.G. Farser, B.D. Marmion (Eds), *Practical Medical Microbiology*, Churchill Livingstone, New York (1989).
[18] Ü.Ö. Özmen, G. Olgun. *Spectrochim. Acta, Part A*, **70**, 641 (2008).
[19] M.R. Maurya, S. Khurana, C. Schulzke, D. Rehder. *Eur. J. Inorg. Chem.*, 779 (2001).

[20] R. Gup, B. Kirkan. *Spectrochim. Acta, Part A*, **62**, 1188 (2005).
[21] B.N.B. Raj, M.R.P. Kurup, E. Suresh. *Spectrochim. Acta, Part A*, **71**, 1253 (2008).
[22] G.-C. Xu, L. Zhang, L. Liu, G.-F. Liu, D.-Z. Jia. *Polyhedron*, **27**, 12 (2008).
[23] B. Samanta, J. Chakraborty, S. Shit, S.R. Batten, P. Jensen, J.D. Masuda, S. Mitra. *Inorg. Chim. Acta*, **360**, 2471 (2007).
[24] H. Tezcan, E. Uzluk. *Dyes Pigments*, **77**, 626 (2008).
[25] H. Khanmohammadi, M. Darvishpour. *Dyes Pigments*, **81**, 167 (2009).
[26] B. Singh, P. Srivastava. *Transition Met. Chem.*, **12**, 475 (1987).
[27] Z.H. Abd El-Wahab, M.M. Mashaly, A.A. Salman, B.A. El-Shetary, A.A. Faheim. *Spectrochim, Acta, Part A*, **60**, 2861 (2004).
[28] K. Nakamoto. *Infrared and Raman Spectra of Inorganic and Coordination Compounds*, 3rd Edn, John Wiley & Sons, New York (1977).
[29] E. Katsoulakou, V. Bekiari, C.P. Raptopoulou, A. Terzis, P. Lianos, E.M. Zoupa, S.P. Perlepes. *Spectrochim. Acta, Part A*, **61**, 1627 (2005).
[30] B. Singh, A.K. Srivastav, P. Srivastava. *Transition Met. Chem.*, **13**, 463 (1988).
[31] P.F. Lee, C.-T. Yang, D. Fan, J.J. Vittal, J.D. Ranford. *Polyhedron*, **22**, 2781 (2003).
[32] L.K. Gupta, U. Bansal, S. Chandra. *Spectrochim. Acta, Part A*, **66**, 972 (2007).
[33] P.N. Remya, C.H. Suresh, M.L.P. Reddy. *Polyhedron*, **26**, 5016 (2007).
[34] W.J. Geaey. *Coord. Chem. Rev.*, **7**, 81 (1971).
[35] M.F.R. Fouda, M.M. Abd-Elzaher, M.M. Shakdofa, F.A. El-Saied, M.I. Ayad, A.S. El-Tabl. *J. Coord. Chem.*, **61**, 1983 (2008).
[36] N.M. Rageh, A.M. Abdel Mawgoud, H.M. Mostafa. *Chem. Papers*, **53**, 107 (1999).
[37] R. Gup, E. Giziroglu, B. Kirkan. *Dyes Pigments*, **73**, 40 (2007).
[38] A.B.P. Lever. *Inorganic Electronic Spectroscopy*, Elsevier, Amsterdam (1968).
[39] R.N. Jadeja, J.R. Shah. *Polyhedron*, **26**, 1677 (2007).
[40] A.M.B. Bastos, J.G. Da Silva, P.I.D.S. Maia, V.M. Deflon, A.A. Batista, A.V.M. Ferreira, L.M. Botion, E. Niquet, H. Beraldo. *Polyhedron*, **27**, 1787 (2008).
[41] B. Graham, L. Spiccia, B.W. Skelton, A.H. White, D.C.R. Hockless. *Inorg. Chim. Acta*, **358**, 3974 (2005).
[42] R.C. Khulbe, R.P. Singh, Y.K. Bhoon. *Transition Met. Chem.*, **8**, 59 (1983).
[43] S.X. Hui, Y.X. Zeng, L. Cun, X.R. Gen. *Transition Met. Chem.*, **20**, 191 (1995).
[44] K.R. Krishnapriya, M. Kandaswamy. *Polyhedron*, **24**, 113 (2005).
[45] G.G. Mohamed, N.E.A. El-Gamal. *Spectrochim. Acta, Part A*, **60**, 3141 (2004).
[46] N. Kabay, E. Erdem, R. Kilinçarslan, E.Y. Sari. *Transition Met. Chem.*, **32**, 1068 (2007).
[47] R. Sharma, S.K. Agarwal, S. Rawat, M. Nagar. *Transition Met. Chem.*, **31**, 201 (2006).
[48] M. Tiliakos, P. Cordopatis, A. Terzis, C.P. Raptopoulou, S.P. Perlepes, E.M. Zoupa. *Polyhedron*, **20**, 2203 (2001).
[49] P. Viswanathamurthi, N. Pharmaraj, S. Anuradha, K. Natarajan. *Transition Met. Chem.*, **23**, 337 (1998).
[50] J.B. Gandhi, N.D. Kulkarni. *Transition Met. Chem.*, **26**, 96 (2001).
[51] N. Raman, D. Raja, A. Sakthivel. *J. Chem. Sci.*, **119**, 303 (2007).
[52] A. Sarkar, S. Pal. *Polyhedron*, **25**, 1689 (2006).
[53] K.B. Gudasi, R.S. Vadavi, R.V. Shenoy, S.A. Patil, M. Nethaji. *Transition Met. Chem.*, **31**, 374 (2006).
[54] A.S. El-Tabl. *Bull. Korean Chem. Soc.*, **25**, 1 (2004).
[55] B.J. Hathaway, D.E. Billing. *Coord. Chem. Rev.*, **5**, 143 (1970).
[56] A.S. El-Tabl. *Transition Met. Chem.*, **27**, 166 (2002).
[57] A.S. El-Tabl. *Transition Met. Chem.*, **21**, 428 (1996).
[58] A.A.G. Tomlinson, B.J. Hathaway. *J. Chem. Soc. A*, 1685 (1968).
[59] A.S. El-Tabl. *Transition Met. Chem.*, **23**, 63 (1998).
[60] A.S. El-Tabl. *Transition Met. Chem.*, **22**, 400 (1997).
[61] R.K. Ray, G.B. Kauffman. *Inorg. Chim. Acta*, **174**, 237 (1990).
[62] R.K. Ray, G.B. Kauffman. *Inorg. Chim. Acta*, **174**, 257 (1990).
[63] I.M. Procter, B.J. Hathaway, P.N. Nicholls. *J. Chem. Soc. A*, 1678 (1969).
[64] D. Kivelson, R. Neiman. *J. Chem. Phys.*, **35**, 149 (1961).
[65] M.C.R. Symons. *Chemical and Biochemical Aspects of Electron Spin Resonance*, Van Nostrand Reinhold, Wokingham (1979).
[66] A.S. El-Tabl, F.A. El-Saied, A.N. El-Hakimi. *J. Coord. Chem.*, **61**, 2380 (2008).
[67] K.M. Ibrahim, I.M. Gabr, R.R. Zaky. *J. Coord. Chem.*, **62**, 1100 (2009).
[68] V.P. Singh, A. Katiyar, S. Singh. *J. Coord. Chem.*, **62**, 1336 (2009).
[69] G.B. Bagihalli, S.A. Patil. *J. Coord. Chem.*, **62**, 1690 (2009).
[70] A. Kulkarni, P.G. Avaji, G.B. Baghialli, S.A. Patil, P.S. Badami. *J. Coord. Chem.*, **62**, 481 (2009).
[71] K.V. Sharma, V. Sharma, R.K. Dubey, U.N. Tripathi. *J. Coord. Chem.*, **62**, 493 (2009).
[72] K.V. Sharma, V. Sharma, R.K. Dubey, U.N. Tripathi. *J. Coord. Chem.*, **62**, 506 (2009).